LA-UR-18-29547 (Accepted Manuscript)

Electric-field tuning of a planar terahertz metamaterial based on strained SrTiO3 layers

Chen, Houtong
Kadlec, Christelle
Skoromets, Volodymyr
Kadlec, Filip
Nemec, Hynek
Jurka, Vlastimil
Hruska, Karel
Kuzel, Petr

To be published in: Journal of Physics D: Applied Physics

DOI to publisher's version: 10.1088/1361-6463/aaa315

Permalink to record: http://permalink.lanl.gov/object/view?what=info:lanl-repo/lareport/LA-UR-18-29547

Electric-field tuning of a planar terahertz metamaterial based on strained $SrTiO_3$ layers

Christelle Kadlec[1], Volodymyr Skoromets[1], Filip Kadlec[1], Hynek Němec[1], Hou-Tong Chen[2], Vlastimil Jurka[1], Karel Hruška[1], Petr Kužel[1]

[1] Institute of Physics, Czech Academy of Sciences, Na Slovance 2, 182 21 Prague 8, Czech Republic

[2] Center for Integrated Nanotechnologies, Los Alamos National Laboratory, Los Alamos, New Mexico 87545, USA

E-mail: kadlecch@fzu.cz, chenht@lanl.gov

Abstract. We demonstrate a metamaterial exhibiting a frequency-tunable response in the terahertz domain, controlled by a bias electric field. The active part of the metamaterial consists of a periodic metallic pattern deposited on a thin epitaxially strained strontium titanate film. The role of the metallic structure is two-fold: it gives rise to the metamaterial resonance and it enables applying an electric bias to the strontium titanate layer. The strained film exhibits a pronounced dependence of its permittivity on the bias, which exerts a strong influence on the resonance. Specifically, the resonance of our structure occurs near 0.5 THz and, upon applying a bias voltage of 55 V, a relative tunability of the resonance frequency of 19% was achieved at room temperature.

PACS numbers: 77.55.fp, 78.67.Pt

Keywords: Tunable metamaterial, metasurfaces, strontium titanate, epitaxial thin films, terahertz waves

Submitted to: *Journal of Physics D: Applied Physics*

The development of tunable devices is still a significant challenge for the evolving terahertz (THz) technology [1, 2]. Components allowing agile manipulation of THz radiation, together with efficient and cost-effective emitters and sensitive detectors, are expected to greatly enhance the versatility of future applications. The development of metamaterials and metasurfaces [3, 4, 5, 6, 7] represents a promising opportunity allowing efficient control of THz radiation [8, 9, 10, 11, 12]. The resonant response of metamaterials can be tuned by reconfiguring their geometry [13, 14], or by varying the metamaterial environment or an active part of the resonant structure [15]. Modifying the conductivity of semiconductor substrates was the first way to tune metamaterials in the THz range through optical excitation [16] or voltage bias [17]. Broadband modulation of transmission via an electric field was achieved through integrating Schottky diodes [18] or high-electron-mobility transistor (HEMT) [19], demonstrating modulation depths up to 80% at MHz modulation rates [20, 21] and even approaching GHz range [19]. Hybrid graphene metamaterials [22, 23] have also enabled a 50–60% modulation depth and tens of MHz modulation speed, owing to an electrostatic tunable carrier density and conductivity in the graphene layer. These devices have demonstrated good performance, however, the majority of them have been focusing on electrically *switchable* resonant response. Electrically *frequency-tunable* metamaterials are highly desirable for many applications but they remain elusive in the THz frequency range.

Resonance frequency tuning is essentially accomplished through actively/dynamically changing the effective capacitance or inductance of a resonator. Tuning of the permittivity [24, 25, 26, 27, 28, 29, 30, 31] of the resonator background environment provides a promising approach to control the value of resonator capacitance. One possible direction relies on employing liquid crystals as the active medium [25, 26, 27, 28]. Another approach makes use of the fact that the permittivity of phase-change materials such as germanium telluride (GeTe) strongly depends on their crystallization state. Thus, the response of THz metamaterials containing GeTe significantly changes with temperature [29]. Less dramatic but easily reversible changes occur using a ferroelectric crystal as an active component, e.g., strontium titanate ($SrTiO_3$). Its temperature-dependent dielectric permittivity results in significant thermal tunability of the THz metamaterial resonance frequency [30, 31]. Such thermally tunable metamaterials are suitable, e.g., for temperature sensing, but inappropriate for a fast modulation of THz beams. However, ferroelectric materials may enable also electrical tuning, as we show below.

A ferroelectric compound of the displacive type features a low-frequency polar phonon, so-called soft mode, which drives the ferroelectric phase transition [32]. Close to the Curie temperature, the soft mode is usually located in the THz range and it significantly contributes to the material permittivity in the whole spectral range below its frequency. Moreover, the strongly anharmonic character of the soft mode close to the phase transition allows for controlling its frequency (and, consequently, the material permittivity) by applying an electric bias [33]. It is worth stressing that the applied bias induces displacements of bound charges only, and it does not cause macroscopic charge currents in the ferroelectric, featuring the advantages of fast tuning, low power

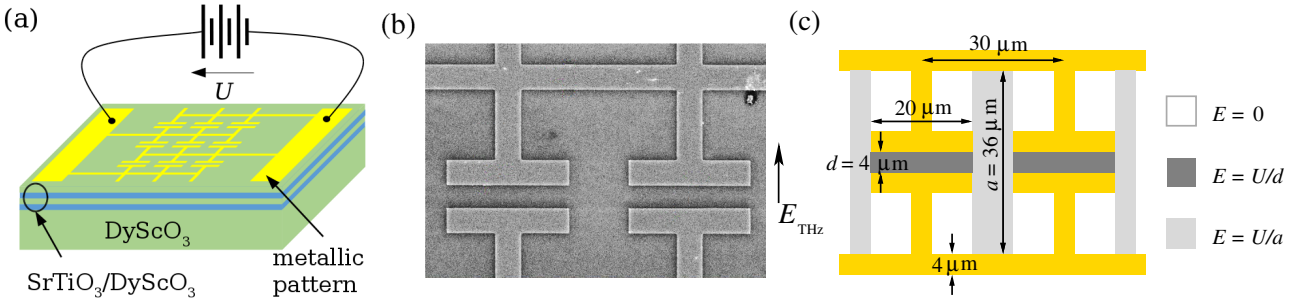

Figure 1. (a) Schematic view of the frequency-tunable THz metamaterial structure. Two $SrTiO_3/DyScO_3$ epitaxial bilayers are deposited on a single-crystal (110) $DyScO_3$ substrate, and the patterned metallic resonators on top of the heterostructure also serve as electrodes. (b) SEM image of the fabricated metamaterial structure. (c) Diagram of the top view with a dc bias applied to the electrodes. The shaded areas mark parts with different field intensities, for which appropriate permittivity spectra $\varepsilon(E)$ corresponding to field values of 0, $E = U/d$, and $E = U/a = U/9d$ were used in the simulations.

consumption, and minimal Joule heating.

As most ferroelectric materials exhibit a strong absorption in the THz spectral range, thin ferroelectric layers are preferred for THz applications. In the present work, we selected a strained $SrTiO_3$ thin film as the tunable ferroelectric layer. Bulk $SrTiO_3$ is an incipient ferroelectric [34] featuring a ferroelectric soft mode but remaining in the paraelectric phase down to the absolute zero. In contrast, $SrTiO_3$ films epitaxially grown on $DyScO_3$ exhibit a tensile strain of ca. 1% with an in-plane spontaneous polarization in the ferroelectric phase. They then undergo the ferroelectric phase transition close to room temperature [35] accompanied by a high permittivity in the THz range which depends on the applied bias [36].

Here we show a proof-of-principle demonstration of a room-temperature electrically frequency-tunable THz metamaterial, schematically shown in Fig. 1(a), based on such strained $SrTiO_3$ thin films. They are embedded into a heterostructure consisting of two $SrTiO_3$ – $DyScO_3$ bilayers grown on a $10 \times 10 \times 0.85\,mm^3$ (110)-oriented single-crystal $DyScO_3$ substrate. This sequence of bilayers with a total $SrTiO_3$ thickness of 100 nm exhibits so far the best tunability at room temperature among those investigated in Ref. [36, 37]. The in-plane periodic resonator array, with a scanning electron microscopy (SEM) image shown in Fig. 1(b), was fabricated on the top of the heterostructure through electron-beam lithography, vacuum metal evaporation (5-nm-thick Cr and 100-nm-thick Au), and a lift-off process. All resonators in one row are interconnected by stripes perpendicular to the THz electric field. The bias voltage U applied to the stripes affects mainly the $SrTiO_3$ permittivity in the capacitive gap, where it induces an electric field intensity $E = U/d$; in addition, a part of the ferroelectric material between the stripes experiences a weaker electric field [$U/a \approx E/9$, see Fig. 1(c)]. By controlling the $SrTiO_3$ permittivity, the bias electric field influences the capacitance of the resonators and it therefore shifts their resonance frequency.

The experiments were performed using a standard THz time-domain spectrometer powered with a Ti:sapphire femtosecond laser oscillator (Coherent, Mira). For the generation of linearly polarized THz pulses we used a biased-semiconductor emitter (TeraSED, GigaOptics); for their detection we applied the usual electro-optic sampling scheme with a 1-mm thick [110] ZnTe crystal. The measurements were performed in the transmission geometry under normal incidence in a helium flow cryostat (Optistat, Oxford Instruments) equipped with electrical lead-through connections to apply the bias. The complex THz transmission spectra of the metamaterial were determined as ratios of Fourier transforms of time-domain waveforms transmitted through the sample with the (biased) THz metamaterial and through a reference $DyScO_3$ substrate with identical crystallographic orientation and a similar thickness.

The room temperature THz transmission spectra of the metamaterial [Fig. 2(a)] display a broad resonance around 0.5 THz, where the $SrTiO_3$ film is highly tunable and the imaginary part of the permittivity significantly decreases under an applied field [36]. This is shown by the significant blue-shift of the metamaterial resonance with increasing applied bias. Reliable estimates of the resonance frequencies were obtained from polynomial fits of the amplitude spectra around the minima (Fig. 3)—the resonance shifts from 0.48 THz at zero bias to 0.57 THz at 55 V, i.e., the relative tunability reaches 19%. The metamaterial resonance tuning manifests itself also by a large variation in the transmission phase—a change exceeding 0.6 rad at 0.5 THz is achieved despite the sub-micron thickness of the structure [Fig. 2(b)]. The Q-factor is relatively low due to the design of the metamaterial structure and the losses in the strained $SrTiO_3$ thin film. It follows that a narrower resonance would require an additional reduction of the dielectric losses of the tunable film, and an improved metamaterial structural design (e.g., using split-ring resonators or asymmetric resonators with Fano-type resonances) with a reduced effective capacitance. It might be also helpful to remove the $SrTiO_3$ thin film except for the gap region to further reduce the losses. The metamaterial structure exhibits no hysteresis for bias voltages up to the value of 55 V. This implies absence of slow processes, which would otherwise limit the operation speed of the device. Note, however, that a hysteresis was observed in a similar $SrTiO_3/DyScO_3$ layer covered by straight interdigital electrodes [38]. In the present device, only small areas are subject to the intense bias, which seems to prevent hysteresis phenomena.

Theoretical calculations were carried out using the finite-element method (Comsol Multiphysics). The permittivity of the unbiased strained $SrTiO_3$ film entering the calculations was determined using a model where the polar soft mode is coupled to a silent low-frequency relaxation, so-called central mode:

$$\varepsilon(\omega) = \varepsilon_\infty + \frac{f}{\omega_0^2 - \omega^2 - \mathrm{i}\omega\Gamma - \delta^2/(1 - \mathrm{i}\frac{\omega}{\gamma})}, \tag{1}$$

where $\omega_0 = 46\,\mathrm{cm}^{-1}$ and $\Gamma = 55\,\mathrm{cm}^{-1}$ are the room temperature soft-mode frequency and damping, respectively, $f \approx 2.34 \times 10^6\,\mathrm{cm}^{-2}$ is the oscillator strength of the soft mode, $\delta = 34\,\mathrm{cm}^{-1}$ is the coupling strength between the soft and central modes, $\gamma = 10\,\mathrm{cm}^{-1}$ is the damping of the central mode, and $\varepsilon_\infty \sim 10$ is the high-frequency

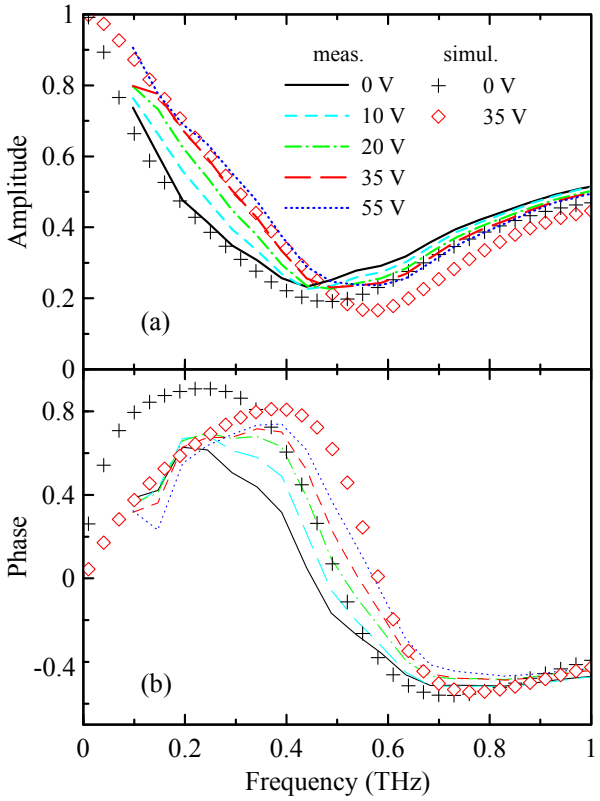

Figure 2. (a) Amplitude and (b) phase of the transmission spectra of the metamaterial for different applied voltages at room temperature (lines: experiment; symbols: simulations)

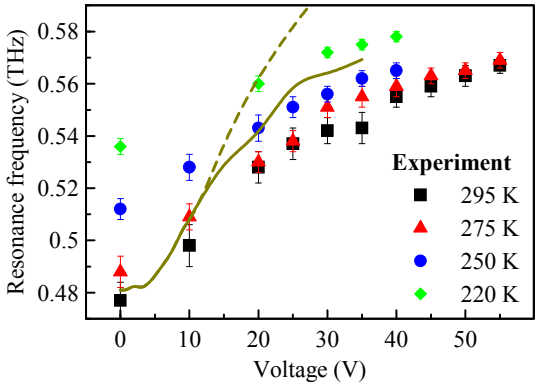

Figure 3. Symbols: measured resonance frequency of the metamaterial as a function of the applied voltage for several temperatures. Lines: resonance frequencies at 295 K determined as the minima of transmission spectra from finite-element calculations, where the $SrTiO_3$ permittivity was modeled by Eq. (1), and the $\omega_0(E)$ values were taken from earlier measurements (Ref. [36], solid line) or assuming an approximate quadratic expansion (dashed line) given by Eq. (2); see also Fig. 4.

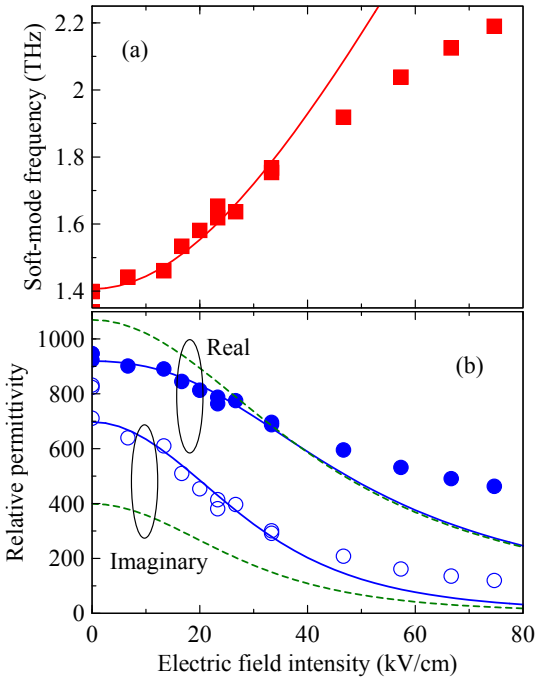

Figure 4. (a) Frequency of the $SrTiO_3$ soft mode at room temperature as a function of the electric field intensity (after [36]). Symbols: measured soft mode frequency; line: approximation in the weak-field limit [Eq. (2)]. (b) Real and imaginary parts of $SrTiO_3$ permittivity at 0.5 THz, calculated using Eq. (1). Symbols: calculations using the measured soft mode frequencies. Solid lines: calculations using the weak-field approximation of the soft mode frequency. Dashed lines: the coupling between the central and soft modes was omitted [$\delta = 0$ in Eq. (1)].

dielectric constant [36]. The soft mode frequency and damping rate depend on the strength of the electric field bias. In simulations we used either the experimental values obtained earlier [36] or based on Eq. (2) below. The results obtained from numerical simulations are also plotted in Fig. 2, revealing good agreement with those obtained from experiments. We find that the tunability of the resonant structure stems essentially from the permittivity changes in the capacitive gaps, while the role of the larger areas with the lower field ($E/9$) is negligible. The reason for this behavior is two-fold. Firstly, the electric field intensity in the large areas is too weak to lead to any substantial change in the permittivity. Secondly, the THz field is concentrated near the capacitive area, thus enhancing the interaction with the part of the structure which exhibits the largest tunability.

For applied voltages below $\sim$15 V (field intensity in the capacitive gap $E \lesssim 35\,\mathrm{kV/cm}$), the soft-mode frequency increases with E^2 [36]:

$$\omega_0(E) = \omega_0(0)\sqrt{1 + 3\beta\left[\frac{\varepsilon_{\mathrm{vac}} f}{\omega_0^2(0)}\right]^3 E^2}, \qquad (2)$$

where $\beta = 2\times10^{10}\,\mathrm{J\cdot C^{-4}m^5}$ is the anharmonic coefficient [37] and $\varepsilon_{\mathrm{vac}}$ is the permittivity of vacuum. In turn, the $SrTiO_3$ permittivity (Fig. 4) and metamaterial resonance

frequency (Fig. 3) also change with E^2. For very low voltages ($U \lesssim 5$ V, $E \lesssim 12\,\mathrm{kV/cm}$), the influence of the E^2-term is marginal and the tuning is thus negligible. Tunability emerges only at higher fields—the soft mode shifts from 1.4 to 1.8 THz when U increases from 5 to 15 V, but the metamaterial resonance shifts only by 7.5%. This is because the soft mode in strained $SrTiO_3$ films is coupled to the silent central mode which, for $\omega > \gamma$, enhances the effective damping of the soft mode, thus inducing a decrease in the permittivity and increase in losses. The influence of the soft-mode–central-mode coupling weakens with increasing soft-mode frequency (Fig. 4). This coupling also leads to a substantial reshaping of the permittivity spectrum upon a shift of the soft mode – the consequence is a change in the resonance spectral profile with increasing bias voltage (Fig. 2).

For applied voltages between 15 and 40 V ($35\,\mathrm{kV/cm} \lesssim E \lesssim 100\,\mathrm{kV/cm}$), the resonance frequency shifts by 7.7%. In this regime, the soft mode frequency no longer shifts with E^2, but its dependence on the electric field intensity becomes sub-linear (Fig. 4), which reduces the tunability of the metamaterial. The influence of the soft-mode–central-mode coupling on the real part of permittivity is negligible for these voltages ($E \gtrsim 30\,\mathrm{kV/cm}$). The tunability of the resonance further decreases at higher applied voltages ($U \gtrsim 40$ V, $E \gtrsim 100\,\mathrm{kV/cm}$). This indicates that the $SrTiO_3$ layers approach the regime where the soft mode is no longer tunable by the external electric field—such a regime was indeed observed in strained $SrTiO_3$ layers [38].

In order to extend our knowledge of the tuning abilities of the THz metamaterial sample, we also measured the voltage-dependent THz transmission at lower temperatures (Fig. 3). The observed behavior is qualitatively similar to that at room temperature. The soft mode frequency increases with decreasing temperature (from 1.4 THz at room temperature to 2 THz at 220 K) [37], which results in a weaker electric-field-induced change in $SrTiO_3$ permittivity around 0.5 THz. For example, the tunability of the transmission between 0 and 40 V drops from 15% at room temperature down to 7.5% at 220 K. This confirms that the best tunability is achieved close to the ferroelectric phase transition, which occurs at room temperature for this particular strained $SrTiO_3$ film [37].

In summary, we have demonstrated a frequency-tunable metamaterial in the THz range, consisting of metallic subwavelength resonators patterned on an active thin layer of strained $SrTiO_3$, where the metallic structure also serves as electrodes for applying a bias voltage. The metamaterial exhibits a resonance near 0.5 THz, which is determined both by the geometric shape of the resonators and by the permittivity of the active layer. Applying a bias has a pronounced influence on the frequency of the ferroelectric soft mode in $SrTiO_3$, which has a direct impact on its permittivity, thus ensuring the tunability of the metamaterial resonance frequency. The tunability of the metamaterial is the highest at room temperature, where the ferroelectric phase transition of $SrTiO_3$ occurs. The tuning curve shows the steepest slope around 10 V, and the resonance frequency can be tuned by up to 19% when the applied voltage increases from 0 to 55 V.

Acknowledgments

This work was supported by the Czech Science Foundation under the project No. 14-25639S, and performed, in part, in the Center for Integrated Nanotechnologies.

References

[1] T. Nagatsuma, G. Ducournau, and C. C. Renaud. Advances in terahertz communications accelerated by photonics. *Nat. Photonics*, 10(6):371–379, 2016.

[2] P. H. Siegel. Terahertz technology in biology and medicine. *IEEE Trans. Microwave Theory Tech.*, 52(10):2438–2447, 2004.

[3] D. R. Smith, J. B. Pendry, and M. C. K. Wiltshire. Metamaterials and negative refractive index. *Science*, 305(5685):788–792, 2004.

[4] W. Cai and V. Shalaev. *Optical Metamaterials: Fundamentals and Applications*. Springer-Verlag, Heidelberg, 2010.

[5] N. F. Yu and F. Capasso. Flat optics with designer metasurfaces. *Nat. Mater.*, 13(2):139–150, 2014.

[6] S. B. Glybovski, S. A. Tretyakov, P. A. Belov, Y. S. Kivshar, and C. R. Simovski. Metasurfaces: From microwaves to visible. *Phys. Rep.*, 634:1–72, 2016.

[7] H.-T. Chen, A. J. Taylor, and N. Yu. A review of metasurfaces: Physics and applications. *Rep. Prog. Phys.*, 79(7):076401, 2016.

[8] L. Q. Cong, W. Cao, X. Q. Zhang, Z. Tian, J. Q. Gu, R. Singh, J. G. Han, and W. L. Zhang. A perfect metamaterial polarization rotator. *Appl. Phys. Lett.*, 103(17):171107, 2013.

[9] N. K. Grady, J. E. Heyes, D. R. Chowdhury, Y. Zeng, M. T. Reiten, A. K. Azad, A. J. Taylor, D. A. R. Dalvit, and H.-T. Chen. Terahertz metamaterials for linear polarization conversion and anomalous refraction. *Science*, 340(6138):1304–1307, 2013.

[10] C. M. Watts, D. Shrekenhamer, J. Montoya, G. Lipworth, J. Hunt, T. Sleasman, S. Krishna, D. R. Smith, and W. J. Padilla. Terahertz compressive imaging with metamaterial spatial light modulators. *Nat. Photonics*, 8(8):605–609, 2014.

[11] R. Mendis, M. Nagai, Y. Wang, N. Karl, and D. M. Mittleman. Terahertz artificial dielectric lens. *Sci. Rep.*, 6:23023, 2016.

[12] C.-C. Chang, D. Headland, D. Abbott, W. Withayachumnankul, and H.-T. Chen. Demonstration of a highly efficient terahertz flat lens employing tri-layer metasurfaces. *Opt. Lett.*, 42(9):1867–1870, 2017.

[13] H. Tao, A. C. Strikwerda, K. Fan, W. J. Padilla, X. Zhang, and R. D. Averitt. Reconfigurable terahertz metamaterials. *Phys. Rev. Lett.*, 103(14):147401, 2009.

[14] N. I. Zheludev and E. Plum. Reconfigurable nanomechanical photonic metamaterials. *Nat. Nanotechnol.*, 11(1):16–22, 2016.

[15] H.-T. Chen, J. F. O'Hara, A. K. Azad, and A. J. Taylor. Manipulation of terahertz radiation using metamaterials. *Laser Photon. Rev.*, 5(4):513–533, 2011.

[16] W. J. Padilla, A. J. Taylor, C. Highstrete, M. Lee, and R. D. Averitt. Dynamical electric and magnetic metamaterial response at terahertz frequencies. *Phys. Rev. Lett.*, 96(10):107401, 2006.

[17] H.-T. Chen, W. J. Padilla, J. M. O. Zide, A. C. Gossard, A. J. Taylor, and R. D. Averitt. Active terahertz metamaterial devices. *Nature*, 444(7119):597, 2006.

[18] H.-T. Chen, W. J. Padilla, M. J. Cich, A. K. Azad, R. D. Averitt, and A. J. Taylor. A metamaterial solid-state terahertz phase modulator. *Nat. Photonics*, 3(3):148–151, 2009.

[19] Y. Zhang, S. Qiao, S. Liang, Z. Wu, Z. Yang, Z. Feng, H. Sun, Y. Zhou, L. Sun, Z. Chen, X. Zou, B. Zhang, J. Hu, S. Li, Q. Chen, L. Li, G. Xu, Y. Zhao, and S. Liu. Gbps terahertz external modulator based on a composite metamaterial with a double-channel heterostructure. *Nano Lett.*, 15(5):3501–3506, 2015.

[20] H.-T. Chen, S. Palit, T. Tyler, C. M. Bingham, J. M. O. Zide, J. F. O'Hara, D. R. Smith, A. C. Gossard, R. D. Averitt, W. J. Padilla, N. M. Jokerst, and A. J. Taylor. Hybrid metamaterials enable fast electrical modulation of freely propagating terahertz waves. *Appl. Phys. Lett.*, 93(9):091117, 2008.

[21] D. Shrekenhamer, J. Montoya, S. Krishna, and W. J. Padilla. Four-color metamaterial absorber THz spatial light modulator. *Adv. Opt. Mater.*, 1(12):905–909, 2013.

[22] S. H. Lee, M. Choi, T. T. Kim, S. Lee, M. Liu, X. Yin, H. K. Choi, S. S. Lee, C. G. Choi, S. Y. Choi, X. Zhang, and B. Min. Switching terahertz waves with gate-controlled active graphene metamaterials. *Nat. Mater.*, 11(11):936–941, 2012.

[23] P. Q. Liu, I. J. Luxmoore, S. A. Mikhailov, N. A. Savostianova, F. Valmorra, J. Faist, and G. R. Nash. Highly tunable hybrid metamaterials employing split-ring resonators strongly coupled to graphene surface plasmons. *Nat. Commun.*, 6:8969, 2015.

[24] T. Driscoll, H. T. Kim, B. G. Chae, B. J. Kim, Y. W. Lee, N. M. Jokerst, S. Palit, D. R. Smith, M. Di Ventra, and D. N. Basov. Memory metamaterials. *Science*, 325(5947):1518–1521, 2009.

[25] O. Buchnev, J. Wallauer, M. Walther, M. Kaczmarek, N. I. Zheludev, and V. A. Fedotov. Controlling intensity and phase of terahertz radiation with an optically thin liquid crystal-loaded metamaterial. *Appl. Phys. Lett.*, 103(14):141904, 2013.

[26] S. Savo, D. Shrekenhamer, and W. J. Padilla. Liquid crystal metamaterial absorber spatial light modulator for THz applications. *Adv. Opt. Mater.*, 2(3):275–279, 2014.

[27] N. Chikhi, M. Lisitskiy, G. Papari, V. Tkachenko, and A. Andreone. A hybrid tunable THz metadevice using a high birefringence liquid crystal. *Sci. Rep.*, 6:34536, 2016.

[28] L. Wang, S. Ge, W. Hu, M. Nakajima, and Y. Lu. Graphene-assisted high-efficiency liquid crystal tunable terahertz metamaterial absorber. *Opt. Express*, 25(20):23873–23879, 2017.

[29] C. H. Kodama and R. A. Jr. Coutu. Tunable split-ring resonators using germanium telluride. *Appl. Phys. Lett.*, 108(23):231901, 2016.

[30] H. Němec, P. Kužel, F. Kadlec, C. Kadlec, R. Yahiaoui, and P. Mounaix. Tunable terahertz metamaterials with negative permeability. *Phys. Rev. B*, 79(24):241108, 2009.

[31] R. Singh, A. K. Azad, Q. X. Jia, A. J. Taylor, and H.-T. Chen. Thermal tunability in terahertz metamaterials fabricated on strontium titanate single-crystal substrates. *Opt. Lett.*, 36(7):1230–1232, 2011.

[32] M. E. Lines and A. M. Glass. *Principles and applications of ferroelectrics and related materials*. Clarendon Press, Oxford, 1977.

[33] V. Skoromets, F. Kadlec, C. Kadlec, H. Němec, I. Rychetský, G. Panaitov, V. Müller, D. Fattakhova-Rohlfing, P. Moch, and P. Kužel. Tuning of dielectric properties of $SrTiO_3$ in the terahertz range. *Phys. Rev. B*, 84(17):174121, 2011.

[34] O. E. Kvyatkovskii. Quantum effects in incipient and low-temperature ferroelectrics (a review). *Phys. Solid State*, 43(8):1401–1419, 2001.

[35] J. H. Haeni, P. Irvin, W. Chang, R. Uecker, P. Reiche, Y. L. Li, S. Choudhury, W. Tian, M. E. Hawley, B. Craigo, A. K. Tagantsev, X. Q. Pan, S. K. Streiffer, L. Q. Chen, S. W. Kirchoefer, J. Levy, and D. G. Schlom. Room-temperature ferroelectricity in strained $SrTiO_3$. *Nature*, 430(7001):758–761, 2004.

[36] C. Kadlec, F. Kadlec, H. Němec, P. Kužel, J. Schubert, and G. Panaitov. High tunability of the soft mode in strained $SrTiO_3/DyScO_3$ multilayers. *J. Phys.: Cond. Matter*, 21(11):115902, 2009.

[37] V. Skoromets, C. Kadlec, J. Drahokoupil, J. Schubert, J. Hlinka, and P. Kužel. Systematic study of terahertz response of $SrTiO_3$ based heterostructures: Influence of strain, temperature, and electric field. *Phys. Rev. B*, 89(21):214116, 2014.

[38] P. Kužel, C. Kadlec, F. Kadlec, J. Schubert, and G. Panaitov. Field-induced soft mode hardening in $SrTiO_3/DyScO_3$ multilayers. *Appl. Phys. Lett.*, 93(5):052910, 2008.